

Research on NETD Test System of Medical Infrared Thermal Imager Based on CCD Imaging Technology

Miao Cao¹ and Wenjie Cui¹

(1.Changchun University of Science and Technology, Jilin Changchun,130022,
China)
79816540@qq.com

Abstract

Under the conditions that the target and background are bold and the transmission loss in atmosphere between systems is neglected, the SNR of the thermal imaging system, the radiation flux of the target and the NETD expression are derived. On this basis, the NETD test system of the modern infrared thermal imager is studied. The system is constructed by a Newton type reflecting parallel light tube, and the off-axis parabolic reflector is as the main body, which provides infinity infrared observation target for infrared thermal imager being tested. The target is composed of the infrared reticle located at the focus of off-axis parabolic reflector and the high precision temperature blackbody at the back of the reticle. The image of infinity infrared target is displayed on its own screen by the infrared thermal imager. CCD shoots the screen of infrared thermal imager, and NETD value is obtained by processing the camera's video signal. The experimental results show that the accuracy of NETD synthesis can reach 0.03 °C in this paper.

Keywords: NETD; Medical Infrared Thermal Imager, CCD Imaging Technology, SNR

1. Introduction

Medical infrared thermal imager is composed of optical system, infrared detector, signal processing circuit and so on. The radiation flux distribution of the scene is imaged to the focal plane of the optical system, namely the photosensitive surface of the detector. The radiation detector receives the scenery radiation and converts the infrared radiation of the various parts of the scene into electrical signals in turn. The amplified signal is converted into a standard video signal. Finally, the infrared thermography of the measured object is showed on the screen or monitor. The noise equivalent temperature difference (NETD) is the main parameter to reflect the performance of the infrared thermal imager, so it is necessary to develop the modern testing equipment for the performance parameters of the infrared thermal imager.

2. Basic Principles of NETD Testing

The standard test pattern of NETD is shown in Figure 1.1.

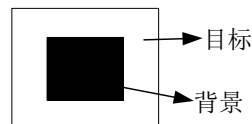


Figure 1.1. The Standard Test Pattern of NETD

A target of uniform temperature is in the background of the assumption that the target and the background are all black. When the system is to observe the test pattern, the peak

signal voltage V_s generated by the system is made to be equal to the RMS noise voltage V_n , that is, the SNR is equal to 1. The temperature difference ΔT between the target and the background is called the system noise equivalent temperature difference, denoted as NETD.

In the actual measurement, in order to ensure the accuracy of measurement, the temperature difference between target and background is usually made larger, so that the signal voltage V_s is several times of the noise voltage V_n , then press the formula:

$$NETD = \frac{\Delta T}{V_s/V_n} \quad (1.1)$$

(1) SNR of thermal imaging system

When there is a temperature difference between the target and the background, the radiation flux from the incident to the thermal imaging system is different, and the signal voltage V_s is:

$$V_s = \Delta\phi_\lambda \cdot R_\lambda \quad (1.2)$$

Where:

R_λ - The response of the detector (V/W)

$\Delta\phi_\lambda$ - Monochromatic radiation difference between the target and the background (W)

Noise RMS voltage V_n of the system is:

$$V_n = \left[\int_0^\infty s'(f) \cdot MTF_e^2 df \right]^{1/2} \quad (1.3)$$

Where:

$s'(f)$ - System noise power spectrum

MTF_e - Electronic filter transfer function

So the SNR of thermal imaging system is:

$$SNR = \frac{V_s}{V_n} = \frac{\Delta\phi_\lambda R_\lambda}{\left[\int_0^\infty s'(f) MTF_e^2 df \right]^{1/2}} \quad (1.4)$$

The noise voltage is within the bandwidth Δf , and the bandwidth of the noise voltage, according to formula (1.2), $V_{n1} \approx [s'(f_0)\Delta f]^{1/2}$ is get. D^*_λ and R_λ relationship:

$$R_\lambda = \frac{D^*_\lambda V_n}{(A_d \cdot \Delta f)^{1/2}} = D^*_\lambda \left[\frac{s'(f_0)}{A_d} \right]^{1/2} \quad (1.5)$$

Formula (1.5) is substituted into (1.6), and SNR is:

$$SNR = \frac{\Delta\phi_\lambda R_\lambda^*}{A_d^{1/2} \left[\int_0^\infty s'(f) MTF_e^2 df \right]^{1/2}} \quad (1.6)$$

Where, $s(f)$ - normalized noise power spectrum, $s(f) = \frac{s'(f)}{s'(f_0)}$

$$\Delta f_n = \int_0^\infty s'(f) MTF_e^2 df \quad (1.7)$$

Define Formula (1.7) as noise equivalent bandwidth. Since the electronic filter of the system is usually low-pass filter,

$$MTF_e = \left[1 + \left(\frac{f}{f_{r0}} \right)^2 \right]^{-1/2}$$

White noise $s(f) = 1$, which the relationship between Δf_n and 3dB frequency f_{i0} is:

$$\Delta f_n = \frac{\pi}{2} f_{i0}$$

From the discussion of the signal processing section, to maintain the pass of basic signal, take $f_{i0} = 1/(2\tau_d)$, so:

$$\Delta f_n = \frac{\pi}{4\tau_d} \tag{1.8}$$

f_{i0} - Dwell time of detector

The formula (1.7) and (1.8) are substituted into (1.6), and:

$$SNR = \frac{\Delta\phi_\lambda D_\lambda^*}{(A_d \Delta f_n)^{1/2}} \tag{1.9}$$

(2) Radiant flux of the target

When no considering the target's reflection on the environment, and setting the target as Lambertian radiator, the targets spectral radiance by Planck's law:

$$L_\lambda = \varepsilon M_\lambda / \pi = \varepsilon \frac{c_1}{\pi \lambda^5} \cdot \frac{1}{\exp\left(\frac{c_2}{\lambda T} - 1\right)} (W \cdot cm^{-2} \cdot \mu m^{-1} \cdot rad^{-1})$$

M_λ -Spectral radiance of the target ($W \cdot cm^{-2} \cdot \mu m^{-1}$)

c_1 -First radiation constant, $c_1 = 3.7415 \times 10^4 (W \cdot \mu m^4 / cm^2)$

c_2 -Second radiation constant, $c_2 = 14388 (\mu m \cdot K)$

ε -Emissivity of the target.

Figure 1.2 shows that the radiation intensity of the target with the area of A_t is $I_\lambda = L_\lambda A_t$, when the target is full of a probe, $A_t = \alpha \cdot \beta \cdot R^2$, then:

$$I_\lambda = L_\lambda \alpha \beta R^2 = \frac{\varepsilon M_\lambda}{\pi} \alpha \beta R^2 (W \cdot rad^{-1} \cdot \mu m^{-1})$$

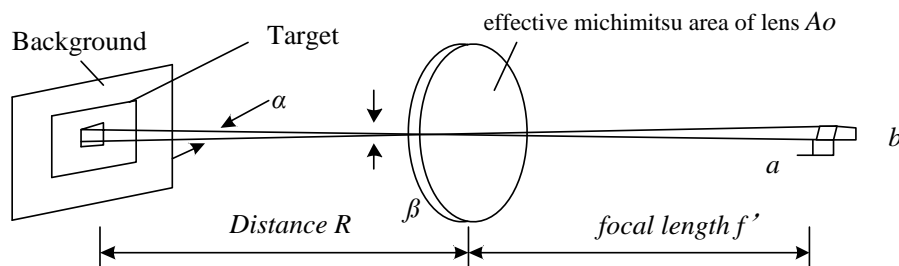


Figure 1.2. Geometrical Relationship Between the Target and Detector

In the system, the angle of the target is $\pi D_0^2 / 4R^2$. D_0 is the pupil diameter e of the optical system. After the atmospheric attenuation of R path and attenuation of the optical system, the radiation flux received by the detector is:

$$\phi_\lambda = \frac{\varepsilon M_\lambda}{4} D_0^2 \alpha \beta \tau_a(\lambda) \tau_0(\lambda) (W / \mu m)$$

Where,

$\tau_a(\lambda)$ -atmosphere spectrum transmission ratio of R path

$\tau_0(\lambda)$ -atmosphere spectrum transmission ratio of optical system

Set the target temperature is T_T , emission rate is ε_T , background temperature is T_B ,

emission rate is ε_B , and the difference of spectral radiant flux between the target and the background on the detector:

$$\Delta\phi_\lambda = \frac{D_0^2}{4} \alpha\beta\tau_a(\lambda)\tau_0(\lambda)[\varepsilon_T M_\lambda(T_T) - \varepsilon_B M_\lambda(T_B)] \quad (1.10)$$

When the difference between T_T and T_B is not big, differentiation can be used to replace difference, so the upper formula can be written as:

$$\Delta\phi_\lambda \approx d\phi_\lambda = \frac{D_0^2}{4} \alpha\beta\tau_a(\lambda)\tau_0(\lambda) \left[\varepsilon_B \frac{\partial M_\lambda(T_B)}{\partial T} \Delta T + \Delta\varepsilon M_\lambda(T_B) \right] \quad (1.11)$$

Where,

ΔT -Temperature difference between target and background

$\Delta\varepsilon$ -Emission rate difference between target and background

(3) NETD expression

Assumptions: Target and background are bold, $\varepsilon_T = \varepsilon_B = 1$. The loss through the atmosphere between the target and the system is negligible, that is, $\tau_a(\lambda) = 1$. $\tau_0(\lambda)$ is constant τ_0 when the system is in the working band.

Thus, the formula (1.11) can be simplified to:

$$\Delta\phi_\lambda = \frac{D_0^2}{4} \alpha\beta\tau_0 \frac{\partial M_\lambda}{\partial T} \Delta T \quad (1.12)$$

The working band of the system is made up of $\lambda_1 \sim \lambda_2$, and the image SNR through Figure 1.9:

$$SNR = \frac{V_s}{V_n} = \Delta T \frac{\alpha\beta D_0^2 \tau_0}{4(A_d \Delta f_n)^{1/2}} \int_{\lambda_1}^{\lambda_2} D_\lambda^* \frac{\partial M_\lambda(T_B)}{\partial T} d\lambda \quad (1.13)$$

The upper formula is just the condition of unit or parallel scan. If serial scan is included, the SNR can be improved by $\sqrt{n_s}$ times. n_s is the number of serial scan. When the thermal imaging system uses a photon detector, its theoretical performance is:

$$\begin{cases} D_\lambda^* = \frac{\lambda D_{\lambda_p}^*}{\lambda_p} & (\lambda \leq \lambda_p) \\ D_\lambda^* = 0 & (\lambda > \lambda_p) \end{cases}$$

Where,

λ_p -The cutoff wavelength determined by the detector material

For medium and long wave infrared radiation, $e^{c_2/\lambda T} \gg 1$, the variation rate of the spectrum radiation to the temperature is approximately:

$$\frac{\partial M_\lambda}{\partial T} \approx \frac{c_2}{\lambda T^2} M_\lambda$$

By substitution of the above two formulas into (1.13), obtained by NETD definition equation:

$$NETD = \frac{\Delta T}{V_s/V_n} = \frac{4F^2 \sqrt{\Delta f_n}}{\sqrt{n_s} \sqrt{A_d} \tau_0 D_{\lambda_p}^*} \left[\frac{c_2}{\lambda_p T_B^2} \int_{\lambda_1}^{\lambda_2} M_\lambda(T_B) d\lambda \right]^{-1} \quad (1.14)$$

Where, F- Number F of the optical system

2. Design of NETD Test System of Infrared Thermal Imager Based on Digital Image Processing

2.1 Overall Scheme Design

In this paper, the system is constructed by a Newton type reflecting parallel light tube, with the off-axis parabolic reflector as the main body, which provides infinity infrared observation target for infrared thermal imager being tested. The target is composed of the infrared reticle located at the focus of off-axis parabolic reflector and the high precision temperature blackbody at the back of the reticle. The image of infinity infrared target is displayed on its own screen through the infrared thermal imager. If it has a video signal output port, the video signal is analyzed and processed by the computer through the video capture card, to obtain the NETD parameters. If there is no video signal output port, CCD will shoot the screen of infrared thermal imager. The camera's video signal can be processed to obtain the relevant performance parameters. The structure of the system is shown in Figure 2.1.

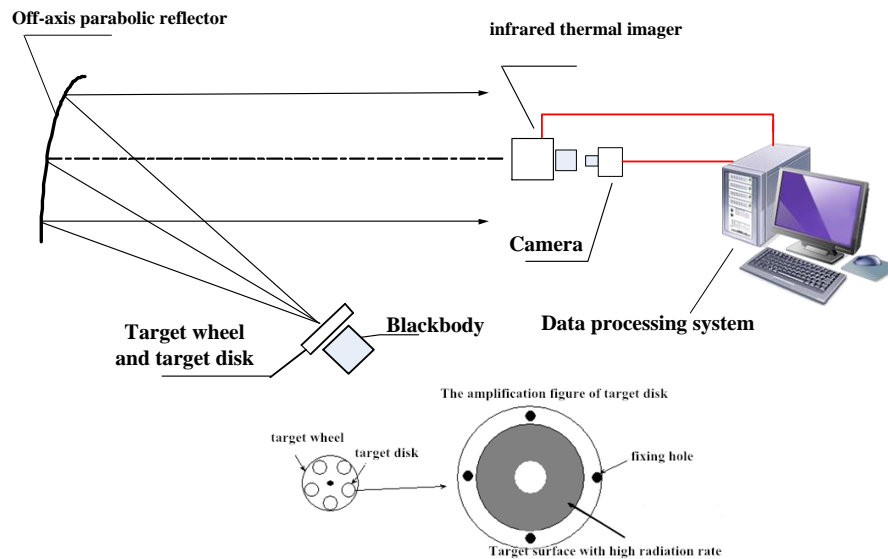


Figure 2.1. The Status of the Instrument Testing NETD

Infrared collimator consists of a face bold, target, off-axis parabolic mirror, and lens barrel which can shelter from stray light and proof dust. The data processing system is composed of the computer, the corresponding board and special software. It is the man-machine interactive medium for the completion of the test operation of the parameters.

When the NETD parameter is tested in the instrument, the target used in the test should be a round target with suitable spatial frequency. The target pattern of the infrared collimator is received by the infrared thermal imager. Firstly, adjust the target temperature difference, so that the brightness of output image is minimal. Record the size of the target temperature difference and output signal at this time.

ΔT is changed so that the temperature difference can be changed from the negative temperature gradually to positive temperature (relative to the target temperature), until the brightness of the hole target becomes saturable. The instrument will record the surface blackbody and the temperature of the target, and process calculation based on the video image of the measured product output. NETD value according to the formula below.

$$NETD(^{\circ}C) = \frac{RMS\ noise\ value(Volts)}{System\ response\ rate(Volts/^{\circ}C)}$$

2.2 Total Experimental Results and Accuracy Analysis

The differential temperature range of the surface blackbody is $-10^{\circ}\text{C}\sim 50^{\circ}\text{C}$, the effective radiating area $\geq \Phi 30\text{mm}$, the temperature resolution of 0.01°C , the temperature control accuracy of $\pm 0.3^{\circ}\text{C}$, the temperature uniformity of $0.1^{\circ}\text{C}(\Delta T \leq \pm 5^{\circ}\text{C}, 2/3$ of the central region). According to functionality and accuracy required, the focal length of off-axis parabolic mirrors $f = 1500\text{mm}$, diameter $D = \Phi 150\text{mm}$, spectral range: $8 \sim 14\mu\text{m}$. With any frame image to measure NETD, the measured results are shown in Table 2.1.

Table 2.1. Test Value and Theoretical Value of NETDT ($^{\circ}\text{C}$)

frame project	1 frame	2 frame	3 frame	4 frame	5 frame
test value	0.048	0.047	0.044	0.049	0.045
theoretical value	0.046	0.046	0.046	0.046	0.046
deviation	0.002	0.001	0.002	0.003	0.001

The main factor that determines the accuracy of the measurement of NETD parameters is the temperature control accuracy of the surface blackbody. And the second is the interpretation accuracy of the digital image interpretation software. The temperature control accuracy of surface blackbody can reach 0.01 . The error caused by the interpretation software can be controlled within 0.02 . The comprehensive test accuracy can reach 0.03°C .

3. Conclusion

As the infrared thermal imager has the advantages of fast response, wide measurement range, and direct measurement results, it has received special attention in the medical field. NETD is the main parameter of the infrared thermal imager. In this paper, the CCD imaging technique is used to study the NETD test system of modern infrared thermal imager. The system is constructed by a Newton type reflecting parallel light tube, the off-axis parabolic reflector is used as the main body, which provides infinity infrared observation target for infrared thermal imager being tested. CCD shoots the screen of infrared thermal imager, and NETD value is obtained by CCD video signal. Experimental results show that the system can measure the NETD value quickly and effectively, and the test precision can reach 0.03°C .

References

- [1] "Night Vision Thermal Imaging System Performance Model User's Manual & Reference Guide", Rev. 5 U.S Army NVESD, (2001).
- [2] L. M. Biberman, "Electro-Optical Imaging System Performance and Modeling, Ch.12", SPIE, Bellingham, WA, (2000).
- [3] B. T. Ting, "Image Edge Detection Based on Wavelet Transform and Canny Operator", Journal of Harbin University of Science and Technology", vol. 15, no. 1, (2010).
- [4] S. Q. Kun, "Improve Fuzzy C - means Clustering Algorithm", Journal of Harbin University of Science and Technology", vol. 12, no. 4, (2007).
- [5] Z. A. Ming, "Sub Pixel Edge Detection Algorithm Based on Quadratic Curve Fitting", Journal of Harbin University of Science and Technology", vol. 11, no. 13, (2006).
- [6] W. Z. Jun and L. J. Yan, "Establishment and Experiment of IR Thermography NDT System", Journal of Harbin University of Science and Technology, vol. 16, no. 2, (2011).